

# Tunable microfluidic optical-fiber devices

Improvements in transmission speeds and capacities of lightwave communication networks typically follow from advances in optics and, often, from progress in the materials science and physics of the optical fiber that forms the backbone of these systems. There are tremendous potential applications of fiber-based devices that can modify, dynamically, the characteristics of optical signals as light passes through the fiber. Many important network operations can be performed in this manner: dynamic chromatic dispersion compensation, programmable adding and dropping of wavelength channels, dynamic gain equalization, and so forth. Tunable fiber devices naturally incorporate the attractive features of optical fiber (i.e. low cost, polarization-independent behavior, etc.) and the well-developed techniques for fiber manipulation (i.e. splicing, terminating, etc.). They also avoid many of the disadvantages—difficult alignment tolerances, challenging reliability requirements, optical coupling inefficiencies, etc.—of components that use bulk optics, waveguides, or microelectromechanical systems, each of which requires light to be coupled out of and back into a fiber.

Existing tunable fiber devices rely almost exclusively on simple thermo-optic and strain-optic effects. The recent introduction of pumped microfluidics into this area provides broad and flexible tuning possibilities.<sup>1,2</sup> This type of photonic device, known as a microfluidic optical fiber ( $\mu$ FF), uses fluidics to manipulate the transmission characteristics of fiber segments whose propagating or leaky modes are sensitive to the optical properties of its surroundings (i.e. the fluids in this case). The  $\mu$ FF devices provide many features—low power, non-mechanical operation, wide tuning range, low insertion loss, polarization independent behavior, etc.—that are attractive for applications in optical networking. A representative  $\mu$ FF design uses planar microfluidic channels that incorporate optical fibers.<sup>2</sup>

Electrowetting phenomena—in which the contact angle of a conductive fluidic droplet can be reversibly adjusted by application of an electrical voltage—can be exploited to move microfluidic plugs into or out of overlap with the fiber. Pumps based on electrowetting provide low-power operation, relatively fast pump-

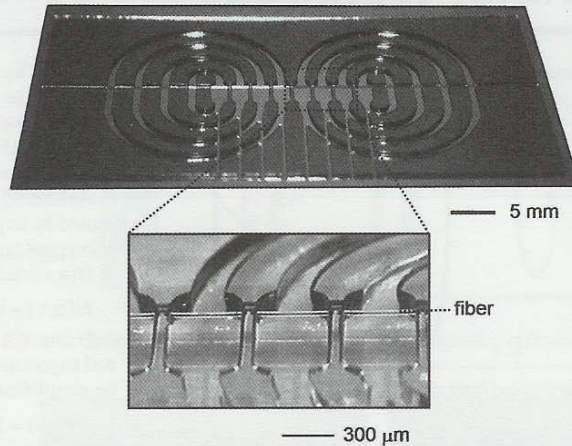


Figure 1. Microchannel structure for a digitally-tunable microfluidic optical fiber device (top). The system consists of eight independent racetrack channels and a mounting slot for the fiber (bottom).

ing speeds, and latchable operation with only a pair of electrodes per pump and no moving parts. In one class of device, a set of discrete microfluidic plugs are individually pumped into or out of overlap with a segment of fiber in a digital manner. Figure 1 shows eight molded plastic recirculating ‘racetrack’ channels to define the flow paths. The fiber mounts into a slot perpendicular to the flow direction. A separate substrate that supports the electrowetting pumps seals against the top surface of the bottom substrate to complete the device. The pumped fluid plugs reside in the short, widened regions of each racetrack.

The electrowetting pumps provide independent control over the positions of the eight plugs (black, as shown in Figure 2). In the up position, the plugs overlap the corresponding segment of optical fiber. In the down position, they are completely out of overlap. Interaction of the plugs with the fiber modifies the transmission characteristics of an in-fiber long-period grating (LPG) designed to create a narrow-band attenuation. In particular, overlap of index matching fluids decreases the strength of this attenuation by an amount proportional to the degree of overlap (i.e. the number of plugs in this case). Figure 3 shows transmission spectra recorded as the number of overlapping plugs increases from one to eight. The different tuning states are achieved reproducibly, in a digital manner, with a switching speed of ~70ms.

One possible application is for dynamic gain equalization (DGE) in wavelength-division-

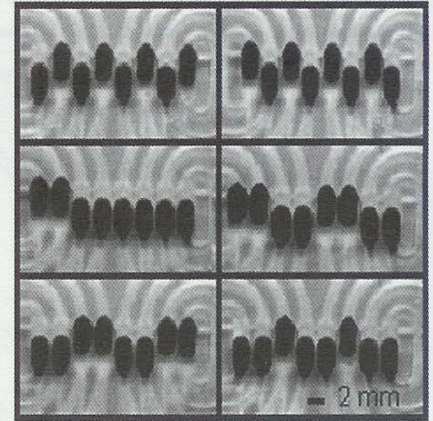


Figure 2. Top view micrographs of a digitally-tunable microfluidic optical fiber device in various tuning states. Electrowetting pumps drive the dark fluidic plugs into or out of overlap with the fiber.

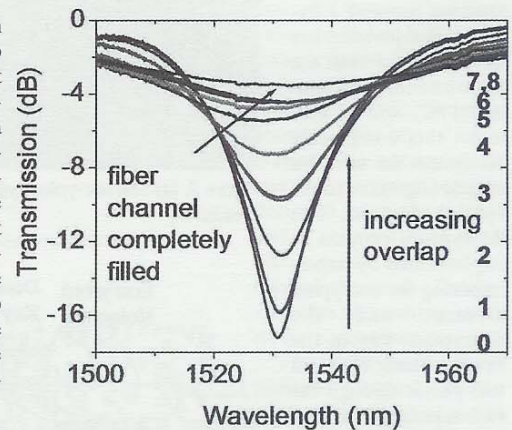


Figure 3. Transmission spectra of a long-period grating (LPG) as eight index-matched fluidic plugs are pumped into overlap with the fiber, sequentially starting with a plug at the edge of the grating (top). The numbers on the right indicate the number of plugs that overlap the grating.

multiplexed communication systems. In this case, a cascaded array of these tunable narrowband filters forms a complex, tunable filter shape that can be adjusted (dynamically) to offset wavelength- (and time-) dependent variations in signal amplification and loss experienced by light passing through the network. Similar fluidic concepts can be used in grating light modulators, lenses, waveguides, and other components.<sup>3-6</sup> This wide range of applications creates interest in pumped microfluidic systems

Continues on page 9.

## Simple optical decryption based on a modified joint-transform correlator technique

Continued from page 4.

$f(x,y)$  and the correlator were simulated to generate the encrypted hologram, while the decryption key  $G(u,v)$  was experimentally shown to recover the encrypted information. The encoded hologram and the decrypted image are shown in Figure 2 (a) and (b) respectively. Using the optical setup shown schematically in Figure 3, the encrypted image was recovered with the decryption key.

For the fabrication of the elements, the number of sampling points was again chosen to be  $128 \times 128$ . Each pixel was  $8 \times 8 \mu\text{m}$  for both holograms, giving a total size of  $1.024 \times 1.024 \text{mm}$ . The holographic patterns were transferred onto pieces of quartz coated with MMA (methyl methacrylate) using electron beam lithography (EBL).

The decoded image is shown in Figure 4: the original image is recovered clearly using the optical decryption key. In the figure, the

bright on-axis spot corresponds to the 0<sup>th</sup>-order diffraction component.

**X.-C. Yuan and S. H. Tao**

Photonics Research Centre  
School of Electrical and Electronic Engineering  
Nanyang Technological University,  
Singapore  
E-mail: excyuan@ntu.edu.sg

### References

1. X.-C. Yuan, S. H. Tao, W. C. Cheong, Y. W. Chen, M. S. Lim, K. J. Moh, and A. T. S. Ho, *Hybrid encryption and decryption technique using microfabricated diffractive optical elements*, **Optical Engineering** **43**, pp. 2493-2494, 2004.
2. R. W. Gerchberg and W. O. Saxton, *A practical algorithm for the determination of phase from image and diffraction plane pictures*, **Optik** **35**, pp. 237-246, 1972.

## Tunable microfluidic optical-fiber devices

Continued from page 3.

for optics, and suggests a bright future for this emerging field of technology.

**John A. Rogers**

University of Illinois  
Urbana, IL  
E-mail: jrogers@uiuc.edu

### References

1. P. Mach, C. Kerbage, M. Dolinski, K. W. Baldwin, R. S. Windeler, B. J. Eggleton, and J. A. Rogers, *Tunable microfluidic optical fiber*, **Appl. Phys. Lett.** **80** (23), p. 4294, 2002.
2. F. Cattaneo, K. Baldwin, S. Yang, T. Krupenkin, S. Ramachandran, and J. A. Rogers, *Digitally tunable microfluidic fiber devices*, **J. Microelectromech. Syst.** **12** (6), p. 907, 2003.
3. O. J. A. Schueller, D. C. Duffy, J. A. Rogers, S. T. Brittain, and G. M. Whitesides, *Reconfigurable diffraction gratings based on elastomeric microfluidic devices*, **Sens. Act. A** **78** (2-3), p. 149, 1999.
5. S. Kuiper and B. H. W. Hendriks, *Variable-focus liquid lens for miniature cameras*, **Appl. Phys. Lett.** **85** (7), p. 1128, 2004.
6. D. B. Wolfe, R. S. Conroy, P. Garstecki, B. T. Mayers, M. A. Fischbach, K. E. Paul, M. Prentiss and G. M. Whitesides, *Dynamic control of liquid-core/liquid-cladding optical waveguides*, **Proc. Nat. Acad. Sci. USA** **101** (34), p. 12434, 2004.

## Design of distortion-invariant optical ID tags

Continued from page 7.

output plane of the recognition system along with the decoded signature obtained for a rotated ( $80^\circ$ ) and scaled version (scale factor 0.7) of the ID tag shown in Figure 1(c). The signature was correctly decoded and identified using nonlinear correlation. To demonstrate the robustness of the ID tags for verification and identification, we recovered the decrypted information from a rotated ( $40^\circ$ ) and scaled (0.8 scale factor) ID tag, and decrypted the encoded information using a false phase key. In this case, we obtained a noisy image with no recognizable signature: See Figure 2(b).

**Elisabet Pérez-Cabré, María S. Millán, and Bahram Javidi\***

Department of Optics and Optometry  
Technical University of Catalonia,  
Barcelona, Spain  
E-mail: eperez@oo.upc.edu

\*Electrical & Computer Engineering  
Department,  
University of Connecticut, Storrs, CT

### References

1. B. Javidi, *Real-time remote identification and verification of objects using optical ID tags*, **Opt. Eng.** **42**, p. 1, 2003.
2. E. Pérez-Cabré and B. Javidi, *Scale and rotation-invariant ID tags for automatic vehicle identification and authentication*, **IEEE Trans. on Vehicular Technology**, accepted for publication, 2005.
3. Ph. Réfrégier and B. Javidi, *Optical image encryption based on input plane and Fourier plane random encoding*, **Opt. Lett.** **20** (7), p. 767, 1995.
4. B. Javidi, *Nonlinear joint power spectrum based optical correlation*, **Appl. Opt.** **28** (12), p. 2358, 1989.

## An input phase mask designed for optical space bandwidth

Continued from page 5.

**Takanori Nomura, Eiji Nitana, Takuhisa Numata, and Bahram Javidi\***

Department of Opto-Mechanics  
Faculty of Systems Engineering  
Wakayama University, Japan  
E-mail: nom@sys.wakayama-u.ac.jp

\*Department of Computer and Systems  
Engineering  
Faculty of Engineering  
University of Connecticut, CT

### References

1. P. Réfrégier and B. Javidi, *Optical image encryption based on input plane and Fourier plane random encoding*, **Opt. Lett.** **20** (7), p. 767, 1995.
2. T. Nomura, et al., *Optical encryption using an input phase mask designed for the space bandwidth of the optical system*, **2004 IEEE LEOS Annual Meeting Conf. Proc.**, p. 344, 2004.
3. T. Nomura, et al., *Design of input phase mask for the space bandwidth of the optical encryption system*, submitted to **Opt. Eng.**